THE BROADBAND SPECTRUM OF CYGNUS X-1

S. Fritz[1], **J. Wilms**[2], **K. Pottschmidt**[3], **M. A. Nowak**[4], **E. Kendziorra**[1], **M. G. Kirsch**[5], **I. Kreykenbohm**[1,6], **and A. Santangelo**[1]

[1]*Institut für Astronomie und Astrophysik, Sand 1, 72076 Tübingen, Germany*
[2]*Dr. Remeis Sternwarte, Astronomisches Institut der Universität Erlangen-Nürnberg, Sternwartstr. 7, 96049 Bamberg, Germany*
[3]*Center for Astrophysics and Space Sciences, University of California, San Diego, La Jolla, CA 92093-0424, USA*
[4]*MIT-CXC, NE80-6077, 77 Massachusetts Ave., Cambridge, MA 02139, USA*
[5]*European Space Astronomy Centre (ESA), Madrid, Spain*
[6]*INTEGRAL Science Data Centre, 16 Ch. d'Ecogia, 1290 Versoix, Switzerland*

ABSTRACT

The Black Hole (BH) binary Cygnus X-1 has been observed simultaneously by *INTEGRAL*, *RXTE*, and *XMM-Newton* for four times in November and December 2004, when Cyg X-1 became first observable with *XMM-Newton*. During these observations the source was found in one of its transitional states between the hard state and the soft state. We obtained a high signal to noise spectrum of Cyg X-1 from 3 keV to 1 MeV which allows us to put constraints on the nature of the Comptonizing plasma by modeling the continuum with Comptonization models as `eqpair` [3]. Using *XMM-Newton* we were also able to confirm the presence of a relativistically broadened Fe Kα line.

Key words: stars: individual (Cyg X-1), black hole physics.

1. INTRODUCTION

Being one of the brightest sources in the X-ray sky, Cyg X-1 has become also one of the best studied Galactic BHs. The system consists of the O9.7I star HDE 226868 of $40 \, M_\odot$ [18] and a compact object with a mass of about $10 \, M_\odot$. Most of the time (90% up to MJD 51300, 75% from then on [17]) the source can be found in its hard state, where the X-ray spectrum is characterized by a power law with photon index $\Gamma \approx 1.7$ and an exponential cutoff at ≈ 150 keV [8, and references therein]. Further spectral characteristics are reflection features from the accretion disk and a relativistically broadened Fe Kα emission line at about 6.4 keV. The other canonical state in which Cyg X-1 can be found is the soft state during which the spectrum is dominated by a soft component peaking at ~ 1 keV followed by a power law tail with index $\Gamma \approx 2 - 3$ [5, 13]. Between these two extremes Cyg X-1 can also be found in the so called "intermediate

Table 1. Observing log for the three instruments used. Times are given in ksec.

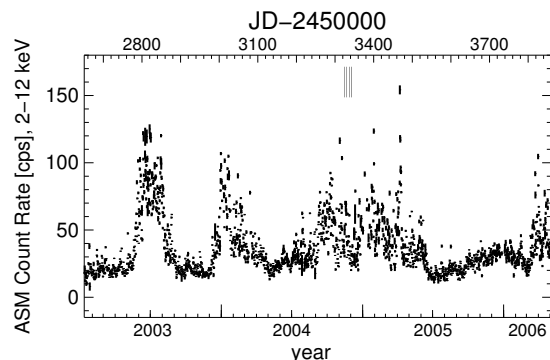| Date	XMM	RXTE	INTEGRAL
14/15 Nov 04 (obs1)	17.6	12.0	58.0
20/21 Nov 04 (obs2)	17.7	16.7	80.0
26/27 Nov 04 (obs3)	20.0	26.0	79.0
02/03 Dec 04 (obs4)	10.0	10.0	80.0

Figure 1. RXTE ASM light curve of Cyg X-1. The vertical lines mark the times of our observations.

states" which exhibit properties of both canonical states [1].

Cyg X-1 was observed in 2004 with *INTEGRAL*, *RXTE*, and *XMM-Newton* simultaneously on November 14/15 (hereafter called obs1), 20/21 (obs2), 26/27 (obs3) and on December 2/3 (obs4). Fig.1 shows the *RXTE/ASM* lightcurve of Cyg X-1 with the four observations indicated by vertical bars. The log of observations is given in Table 1. The observations took place during one of the transitional states of Cyg X-1 which are very interesting for a further study due to the fact that they are characterized by radio flaring, the presence of a relativistically broadened iron line as well as a complex X-ray timing behavior [e.g. 4, 12, 17, 11, 2].

In this contribution we present some results of our on-going analysis. For *RXTE* we used data from the *PCA* and *HEXTE*, covering an energy range from 3 to 120 keV. The data extraction was done using HEA-SOFT 5.3.1. The *INTEGRAL* spectra comprise information of the three instruments *JEM-X*, *IBIS (ISGRI)*, and *SPI*, including energies up to 1 MeV and were reduced using *INTEGRAL* OSA 5.1. The data reduction followed the standard procedures as described in the cookbooks (`http://isdc.unige.ch/?Support+documents`). For *XMM-Newton* we only use data from the EPIC-pn as the EPIC-MOS was switched off to allocate maximum telemetry to the EPIC-pn (see also the paragraph on the Modified Timing Mode below). The energy range used for the *XMM-Newton* analysis is 2.8 to 9.4 keV.

Due to the not yet finalized calibration of the *XMM-Newton* Modified Timing Mode we divide our analysis in two parts. For the first part we combined the *INTEGRAL* and *RXTE* data to study the broadband continuum. The analysis of the relativistically broadened Fe Kα line was done independently using the *XMM-Newton* data only.

2. CONTINUUM

To model the broadband continuum we used the hybrid thermal/non-thermal Comptonization code `eqpair` by [3] which also includes electron-positron pair production. In this model the temperature of the Comptonizing medium is computed self-consistently by balancing Compton cooling with external heating. The amount of heating is specified by the the ratio ℓ_h/ℓ_s of the compactness of the Comptonizing medium and the seed photon distribution. We modeled the soft emission by adding a `diskbb` component which provides the seed photons for the Comptonization (therefore we set the temperature of the `eqpair` seed photons equal to the temperature at the inner edge of the disk). This continuum is partly reflected off the accretion disk (*XSPEC* model `reflect`) and modified at lower energies by interstellar absorption.

We first performed pure thermal `eqpair` fits to the four observations independently [7]. In all cases they showed evidence of a spectral hardening above ≈ 300 keV which could be an indicator for the presence of a non-thermal electron component in the plasma. In order to get better statistics for *SPI* in the crucial energy range we decided to sum up a time averaged spectrum comprising all *INTEGRAL* and *RXTE* observations although Cyg X-1 was highly variable during the observations. For this time averaged spectrum we first considered again a pure thermal plasma. We fixed $\ell_s = 10$ to force the seed photon spectrum to be dominated by disk radiation and assumed a disk inclination of 45 deg [e.g. 9]. As the inner radius of the disk could not be constrained it was fixed to its default value $R_{in} = 10 R_g$. Table 2 shows the best fit parameters. The resulting disk parameters $kT_{in} = 1.10^{+0.03}_{-0.02}$ keV and norm=45^{+7}_{-3} as well as the values for the compactness ratio ($\ell_h/\ell_s = 3.32^{+0.02}_{-0.01}$), the optical depth ($\tau = 1.23^{+0.01}_{-0.01}$),
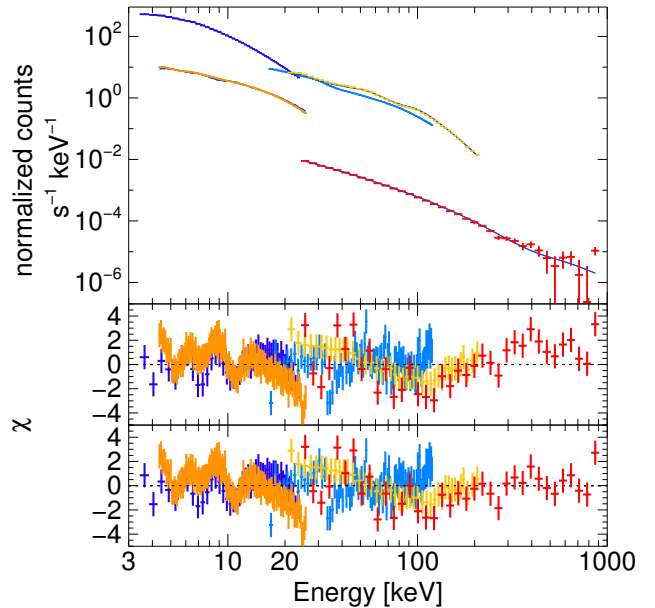

Figure 2. Best fit to the time averaged spectrum using the `eqpair` *model (PCA: 3–25 keV, dark blue; HEXTE: 15–120 keV, light blue; JEM-X: 4–26 keV, orange; IBIS (ISGRI): 20–250 keV, yellow; SPI: 25–1000 keV, red). The upper panel shows the residuals to the pure thermal fit, the lower one those of the hybrid thermal/non-thermal model.*

and the reflection covering factor ($\Omega/2\pi = 0.29^{+0.01}_{-0.01}$) are consistent with the results obtained from analyzing the four observations independently. Also the Iron line parameters match the values obtained before. The χ^2_{red} yields a value of 1.72 with 350 dof. As shown in Fig. 2 a deviation between the data points and this pure thermal model is still present in the time averaged spectrum.

Therefore we added a non-thermal component in the `eqpair` model by allowing the parameter ℓ_{nth}/ℓ_h to vary. We found that 57% of the power supplied to the electrons in the plasma is contained in the non-thermal distribution of the electrons, which was chosen to be a power law (Table 2). This additional component improves the χ^2_{red} to 1.62 (349 dof). The dimensionless parameter ℓ_h/ℓ_s increases to a value of $4.49^{+0.05}_{-0.03}$, $\tau = 1.47^{+0.01}_{-0.01}$ and $\Omega/2\pi = 0.33^{+0.01}_{-0.01}$ are also slightly higher than in the pure thermal model. The disk parameters ($kT_{in} = 1.09^{+0.07}_{-0.03}$ keV and norm=48^{+9}_{-3}) as well as the values found for the Fe Kα line do not change significantly with respect to the thermal model.

3. IRON LINE

3.1. Modified Timing Mode

Due to telemetry restrictions it is not always trivial to study bright sources with the maximum possible time res-

	`eqpair` (th.)	`eqpair` (th./nth.)
N_H [10^{22}cm^{-2}]	$0^{+0.22}_{-0}$	$0^{+0.16}_{-0}$
kT_{in} [keV]	$1.10^{+0.03}_{-0.02}$	$1.09^{+0.07}_{-0.03}$
norm	45^{+7}_{-3}	48^{+9}_{-3}
$E_{K\alpha}$ [keV]	$6.32^{+0.12}_{-0.12}$	$6.32^{+0.05}_{-0.11}$
$\sigma_{K\alpha}$ [keV]	$0.77^{+0.13}_{-0.06}$	$0.72^{+0.12}_{-0.06}$
ℓ_h/ℓ_s	$3.32^{+0.02}_{-0.01}$	$4.49^{+0.05}_{-0.03}$
ℓ_{nth}/ℓ_h	–	$0.57^{+0.02}_{-0.03}$
τ	$1.23^{+0.01}_{-0.01}$	$1.47^{+0.01}_{-0.01}$
$\Omega/2\pi$	$0.29^{+0.01}_{-0.01}$	$0.33^{+0.01}_{-0.01}$
ξ	2^{+7}_{-2}	0^{+19}_{-0}
χ^2_{red} / dof	$1.72 / 350$	$1.62 / 349$

Figure 3. Fit to the obs2 XMM-Newton data. `Upper panel:` *Power-law fit to the data outside the 5–8 keV band. There are strong residuals remaining in the Fe Kα region.* `Lower panel:` *Fit to the whole band using a power-law and a narrow line and a relativistic line.*

olution in combination with a satisfying signal to noise ratio using the standard modes of *XMM-Newton*. In the EPIC-pn burst mode (which is foreseen for very bright sources) only 3% of all detected photons are transmitted resulting in a enormous reduction of the signal to noise ratio. We therefore used an alternative approach which includes switching off the EPIC-MOS camera and running the EPIC-pn in a Modified Timing Mode [10]. In this mode the lower energy threshold was increased to 2.8 keV (the standard value is 200 eV). This implies that a re-calibration of the instrument is required because the combination of split events is not done on-board but during the first step of the EPIC-pn data analysis. Due to the increased lower threshold a large fraction of the split partners is not transmitted and therefore the spectrum appears to be softer. By comparison with former Timing Mode observations we built a new detector response matrix [16]. However, there are still some effects not included yet, for example the improvement of the Charge Transfer Efficiency of the detector due to the high count rates. The special calibration for the Modified Timing Mode will be made public through the *XMM-Newton* SOC as soon as full confidence on the calibration has been reached.

3.2. Relativistically broadened Iron lines

The Fe Kα line observed in BH candidates is intrinsically narrow with a rest frame energy of 6.4–6.97 keV depending on the ionization state. It originates from material which is just a few gravitational radii away from the BH and therefore it is broadened by gravitational redshift effects as well as by Doppler shifts. The exact shape of the
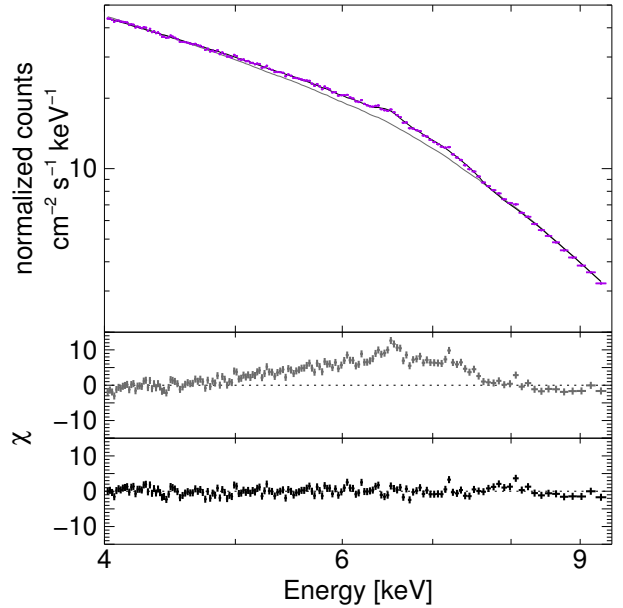
line depends on the accretion geometry, namely on the Fe Kα emissivity of the disk, the angular momentum of the BH and the observer's viewing angle. Relativistically broadened Iron lines are therefore an important observational tool for the understanding of the accretion geometry. For more information on relativistically broadened Iron lines see for example [15, 6].

3.3. Results

Due to the increased soft X-ray emission during the transitional state there is an increased pile-up in the center of the point spread function. We therefore excluded data from the innermost 3 CCD columns from our analysis, however the signal to noise ratio of the data is still sufficient for spectral analysis as could be seen in Fig. 3.

A power-law fit to the *XMM-Newton* data outside the 5–8 keV band reveals strong residuals in the Fe Kα region ($\chi^2_{red} = 21.4$). Modeling these residuals by a narrow ($\sigma = 80 \pm 35$ eV) line at $E = 6.52 \pm 0.02$ keV with an equivalent width of 14 eV and a relativistic Kerr line at $E = 6.76 \pm 0.1$ keV (equivalent width 400 eV) improves the χ^2_{red} dramatically to 1.3. The emissivity of the relativistic line is found to be $\propto r^{-4.3 \pm 0.1}$. These parameters are similar to earlier *Chandra* intermediate state observations by Miller et al. [12]. Note however that the calibration of the timing mode is not yet fully completed so that the energy values obtained from our analysis could be slightly too high.

4. SUMMARY AND OUTLOOK

The 3 keV–1 MeV broadband spectrum of Cyg X-1 can be well described by the `eqpair` model. The parameters we obtain from our analysis are consistent with previous results e.g. from the *RXTE* monitoring campaign [17, 7, 14]. Furthermore our data show evidence for the presence of a non-thermal component in the distribution of the electrons with 57% of the power supplied to the electrons going into the non-thermal acceleration.

The simultaneous *XMM-Newton* observation confirms the presence of a relativistic line [12] during the intermediate state of Cyg X-1 and the parameters obtained for the broad and narrow components lead to the conclusion that the accretion disk seems to extend down to the innermost stable orbit at $1.235\,R_{\rm g}$.

As soon as the calibration of the Modified Timing Mode is completed we will combine all three instruments to model the whole broadband spectrum from 2.8 keV up to 1 MeV.

REFERENCES

[1] T. Belloni. In L. Burderi, L. A. Antonelli, F. D'Antona, T. di Salvo, G. L. Israel, L. Piersanti, A. Tornambè, and O. Straniero, editors, *Interacting Binaries: Accretion, Evolution, and Outcomes*, volume 797 of *American Institute of Physics Conference Series*, pages 197–204, 2005.

[2] M. Cadolle Bel, P. Sizun, A. Goldwurm, J. Rodriguez, P. Laurent, A. A. Zdziarski, L. Foschini, P. Goldoni, C. Gouiffès, J. Malzac, E. Jourdain, and J.-P. Roques. *Astron. Astrophys.*, 446:591–602, 2006.

[3] P. S. Coppi. *Mon. Not. R. Astron. Soc.*, 258:657–683, 1992.

[4] W. Cui, S. N. Zhang, W. Focke, and J. H. Swank. *Astrophys. J.*, 484:383, 1997.

[5] J. F. Dolan, C. J. Crannell, B. R. Dennis, K. J. Frost, and L. E. Orwig. *Nature*, 267:813–815, 1977.

[6] A. C. Fabian. *Astronomische Nachrichten*, 327:943, 2006.

[7] S. Fritz, J. Wilms, K. Pottschmidt, M.A. Nowak, I. Kreykenbohm, and A. Santangelo. In A. Wilson, editor, *Proceedings of the X-ray Universe 2005*, number 604 in ESA SP, pages 267–268, Noordwijk, 2006. ESA Publications Division.

[8] M. Gierliński, A. A. Zdziarski, C. Done, W. N. Johnson, K. Ebisawa, Y. Ueda, F. Haardt, and B. F. Phlips. *Mon. Not. R. Astron. Soc.*, 288:958–964, 1997.

[9] M. Gierliński, A. A. Zdziarski, J. Poutanen, P. S. Coppi, K. Ebisawa, and W. N. Johnson. *Mon. Not. R. Astron. Soc.*, 309:496–512, 1999.

[10] E. Kendziorra, J. Wilms, F. Haberl, M. G. F. Kirsch, M. Martin, and M. A. Nowak. In G. Hasinger and M. J. L. Turner, editors, *Proceedings of the SPIE, Volume 5488*, pages 613–622, 2004.

[11] J. Malzac, P. O. Petrucci, E. Jourdain, M. Cadolle Bel, P. Sizun, G. Pooley, C. Cabanac, S. Chaty, T. Belloni, J. Rodriguez, J. P. Roques, P. Durouchoux, A. Goldwurm, and P. Laurent. *Astron. Astrophys.*, 448:1125–1137, 2006.

[12] J. M. Miller, A. C. Fabian, R. Wijnands, R. A. Remillard, P. Wojdowski, N. S. Schulz, T. Di Matteo, H. L. Marshall, C. R. Canizares, D. Pooley, and W. H. G. Lewin. *Astrophys. J.*, 578:348–356, 2002.

[13] Y. Ogawara, K. Mitsuda, K. Masai, J. V. Vallerga, L. R. Cominsky, J. M. Grunsfeld, J. S. Kruper, and G. R. Ricker. *Nature*, 295:675, 1982.

[14] K. Pottschmidt, J. Wilms, M. A. Nowak, S. Larsson, A. A. Zdziarski, and G. G. Pooley. *Advances in Space Research*, 38:1350–1353, 2006.

[15] C. S. Reynolds and M. A. Nowak. *Phys. Rep*, 377:389–466, 2003.

[16] J. Wilms, E. Kendziorra, M.A. Nowak, K. Pottschmidt, F. Haberl, M. Kirsch, and S. Fritz. In A. Wilson, editor, *Proceedings of the X-ray Universe 2005*, number 604 in ESA SP, pages 217–222, Noordwijk, 2006. ESA Publications Division.

[17] J. Wilms, M. A. Nowak, K. Pottschmidt, G. G. Pooley, and S. Fritz. *Astron. Astrophys.*, 447:245–261, 2006.

[18] J. Ziółkowski. *Mon. Not. R. Astron. Soc.*, 358:851–859, 2005.